A Re-examination of the Portevin-Le Chatelier Effect in Alloy 718 in Connection with Oxidation-Assisted Intergranular Cracking

BERTRAND MAX, BERNARD VIGUIER, ERIC ANDRIEU, and JEAN MARC CLOUE

In Alloy 718, a sharp transition exists in the fracture path changing from an intergranular brittle mode to a transgranular ductile mode which is associated with a transition of flow behavior from smooth in the dynamic strain aging regime to a serrated one in the Portevin-Le Chatelier (PLC) regime. In order to better understand both deformation and rupture behavior, PLC phenomenon in a precipitation-hardened nickel-base superalloy was carefully investigated in a wide range of temperatures [573 K to 973 K (300 °C to 700 °C)] and strain rates (10^{-5} to 3.2×10^{-2} s^{-1}). Distinction was made between two PLC domains characterized by different evolutions of the critical strain to the onset of the first serration namely normal and inverse behavior. The apparent activation energies associated with both domains were determined using different methods. Results showed that normal and inverse behavior domains are related to dynamic interaction of dislocations with, respectively, interstitial and substitutional solutes atoms. This analysis confirms that normal PLC regime may be associated to the diffusion of carbon atoms, whereas the substitutional species involves in the inverse regime is discussed with an emphasis on the role of Nb and Mo.

DOI: 10.1007/s11661-014-2508-6

I. INTRODUCTION

ALLOY 718 is a widely used superalloy for high performance applications because of its excellent mechanical properties over a wide range of temperatures. Nevertheless, alloy 718 is also well known to be sensitive to intergranular stress crack growth.[1,2] This sensitivity to stress corrosion cracking has been observed for various simulated in service conditions for different types of applications (including nuclear power plants and aeronautical industries).[3,4] It was shown that the damaging mechanisms encountered in pressurized water reactors [623 K (350 °C) in water] are similar to the ones found at higher temperature under air [923 K (650 °C) in air].[5] Alloy 718 also exhibits dynamic strain aging (DSA) phenomenon[6–10] related to dynamic interactions between mobile solute atoms and the moving dislocations. Within a limited domain of the temperature *vs* strain rate plane, this DSA results in plastic instabilities called Portevin-Le Chatelier effect, which may often be revealed by the occurrence of serrations on the tensile curve. Despite the fact that PLC domain is obviously a sub-domain of DSA phenomenon, for sake of simplicity we will denote throughout this paper "PLC" the temperature and strain rate ranges in which the plastic instabilities occur and "DSA" the domain without instabilities. Fournier *et al.*,[11] while studying the effect of oxidation on the mechanical behavior of alloy 718 for temperatures ranging from 673 K to 873 K (400 °C to 600 °C) and at a strain rate of 5×10^{-7} s^{-1}, showed that the occurrence of PLC phenomenon during tensile test systematically resulted in the absence of brittle area on the fracture surface of the samples. By contrast when the stress-strain curves are smooth intergranular cracking areas were always observed on the fracture surface. This finding was further confirmed by Garat *et al.*[12] for tensile tests in air at temperatures higher than 673 K (400 °C) and over a wide range of strain rates (10^{-5} to 10^{-3} s^{-1}). These authors showed that the fracture mode domain (intergranular or not) and the deformation mode domain (smooth or serrated) superimpose in the strain rate *vs* temperature plane. The first explanations for such an observation mainly considered the mechanical aspect of the PLC phenomenon. However, the phenomena like the DSA/PLC deformation modes obviously include a "chemical" aspect. For instance Ter-Ovanessian *et al.*[13] evidenced the displacement of PLC domain and the rupture mode domain in the temperature-strain rate plane caused by the diminution of interstitial content of the same heat of alloy 718. These experimental results lead to consider the possibility of a coupling between chemical aspects and mechanical behavior as a possible contribution to explain the relation between rupture mode and deformation mode. In other words, the possible enrichment of grain boundaries during plastic deformation by solute elements that may increase the sensitivity of the material to intergranular cracking has been considered. This enrichment is supposed to occur

BERTRAND MAX, Ph.D. Researcher, BERNARD VIGUIER and ERIC ANDRIEU, Professors, and JEAN MARC CLOUE, Senior Researcher, are with the CIRIMAT, ENSIACET/INP, Université de Toulouse, 4 Allée Emile Monso, BP 44362, 31030 Toulouse Cedex 4, France. Contact e-mail: bernard.viguier@ensiacet.fr
Manuscript submitted January 17, 2014.
Article published online August 14, 2014

by transport of solute species by the dislocations responsible for the plastic deformation in the DSA regime. In this view, a study of the dynamic interactions between solute species and mobile dislocations in the alloy is a good way to access to information about which species are implied. This is the reason why a study of inhomogeneous plastic deformation in alloy 718 was carried out by means of tensile tests.

Inhomogeneous plastic deformation appears in interstitial and substitutional alloys over a wide range of temperatures and strain rates. This phenomenon, also called PLC effect, serrated yielding or jerky flow, has been extensively studied in a great variety of alloys, as reviewed in Reference 14 This plastic behavior is a specific manifestation of the DSA phenomenon which is characterized by sudden stress drops on the plastic part of stress-strain curves called serrations. Since the works of Cottrell,[15,16] the most commonly accepted explanation for this phenomenon lies in the dynamic interaction between diffusing solute atomic species and mobile dislocations during plastic deformation.

Nickel-based superalloys are subject to DSA phenomena, which include, over wide ranges of temperatures and strain rates, the occurrence of PLC effect. Indeed, serrated curves have already been observed and studied in Waspaloy,[6,17] alloy 625,[18,19] Udimet 720,[20,21] Inconel 738,[22] and alloy 718.[6,8–10] The purpose of this paper is to report and share some of the results on the serrated yielding in Alloy 718 in the temperature range 573 K to 973 K (300 °C to 700 °C) and the strain rate range 10^{-5} to 3.2×10^{-2} s^{-1}. The results are discussed with respect to other studies on the alloy.

II. EXPERIMENTAL

Alloy 718 used in the present study was provided in the form of single coil of rolled thin strip (0.64 mm thick) in the solutionized state. The alloy exhibited an homogeneous equiaxed grain structure with mean grain size around 15 to 20 μm. Tensile specimens with gage dimensions $20 \times 3.3 \times 0.64$ mm^3 were cut by laser beam machining. The samples were sealed in Fe-Cr-Al-Y wraps and aged under a vacuum of 5×10^{-5} mbar following the conventional aeronautical heat treatment: 993 K (720 °C)-8 h/893 K (620 °C)-8 h. The edges of the gage lengths of the samples were then mechanically milled by 0.15 mm on each side in order to remove the laser cut heat-affected zone. The final gage dimensions were $20 \times 3.0 \times 0.64$ mm^3. The specimens were tensile tested in air on a screw driven MTS testing machine at constant crosshead velocities corresponding to initial strain rates in the range 10^{-5} to 3.2×10^{-2} s^{-1}. The deformation of the sample was measured *via* laser extensometer. The heating of sample was achieved by a radiation furnace. The temperature on the gage length of the samples was controlled precisely by two K type thermocouples. The specimens were held at the testing temperature 10 minutes before starting the tensile test. The range of temperatures tested was 573 K to 973 K (300 °C to 700 °C). Microstructures and rupture surfaces were characterized by scanning electron microscopy (SEM).

Tensile tests have been carried out on a model alloy without Nb (Alloy 718-Nb). The last elaboration steps of this model alloy consisted in cold rolling down to 0.5 mm thickness and re-crystallization at 1323 K (1050 °C) for 40 seconds, resulting in an equiaxed grain structure. The grains population is not perfectly homogeneous, but the average grain size range from 15 to 30 μm. Tensile specimens with gage dimensions $20 \times 3.3 \times 0.5$ mm^2 were electro discharge machined. Their edges were finally milled by 0.15 mm on each side to remove the heat-affected zone. The final gage dimensions were $20 \times 3.0 \times 0.5$ mm^3.

All tensile specimens were mechanically milled until grade 1200 SiC paper on each surface. The global chemical composition of the alloy as determined by glow discharge mass spectrometry (GDMS)/interstitial gas analysis (IGA) is given in Table I.

III. RESULTS

A. *Microstructure*

Alloy 718 in the field of the present study is a rolled nickel-based superalloy strengthened by precipitation hardening of γ'-Ni_3(Ti, Al) and γ''-Ni_3Nb phases, and, to a lesser extent, by solid solution hardening. The microstructure of the alloy after the standard aeronautical heat treatment consists in a γ-Ni matrix strengthened by a fine distribution of disk-shaped γ''-Ni_3Nb and spherical γ'-Ni_3(Ti,Al) with a total volume fraction of all precipitates around 16 pct. The major strengthening effect is provided by γ'' (80 to 90 pct), which average diameter is generally about 50 nm. The alloy contains also carbide type precipitates dispersed in the matrix or aligned in the rolling direction. As expected following the standard aeronautical heat treatment, the stable Ni_3Nb δ phase could not be detected. Typical microstructure exhibiting equiaxed fully re-crystallized fine grains is shown on Figure 1(a).

The typical microstructure of alloy 718-Nb is shown on Figure 1(b). Alloy 718-Nb has been used in the present study in a solid solution state, as the absence of Nb prevents it from developing γ'' precipitation, which makes it only comparable with solid solution alloy 718.

B. *Experimental Results*

True stress–true strain curves were obtained for the specimens of alloy 718 tested in the temperature range of 573 K to 973 K (300 °C to 700 °C) and the strain rate range of 10^{-5} to 3.2×10^{-2} s^{-1}. Depending on the temperature and the strain rate of the tensile test, the stress-strain curves were either smooth or exhibited serrations. Examples of true stress–true strain curves obtained at $\dot{\varepsilon} = 3.2 \times 10^{-4}$ s^{-1} for different temperatures are presented in Figure 2. As was observed in previous studies,[11–13] fracture surface of specimens exhibiting smooth tensile curve present a partly intergranular brittle characteristics, whereas in the case of

Table I. Chemical Composition (Weight Percent) of the Alloys Used in this Study, as Measured by GDMS-IGA

	Ni	Fe	Cr	Nb	Ta	Al	Mo	Mn	Si	Co	C	B	P	S
Alloy 718	bal.	18.3	18.4	4.94	0.01	0.95	0.56	3.0	0.06	0.02	0.033	0.002	0.005	0.0002
Alloy 718-Nb	bal.	18.5	17.9	<0.001	—	1.01	0.52	2.9	0.119	0.061	0.06	0.0045	0.006	0.0034

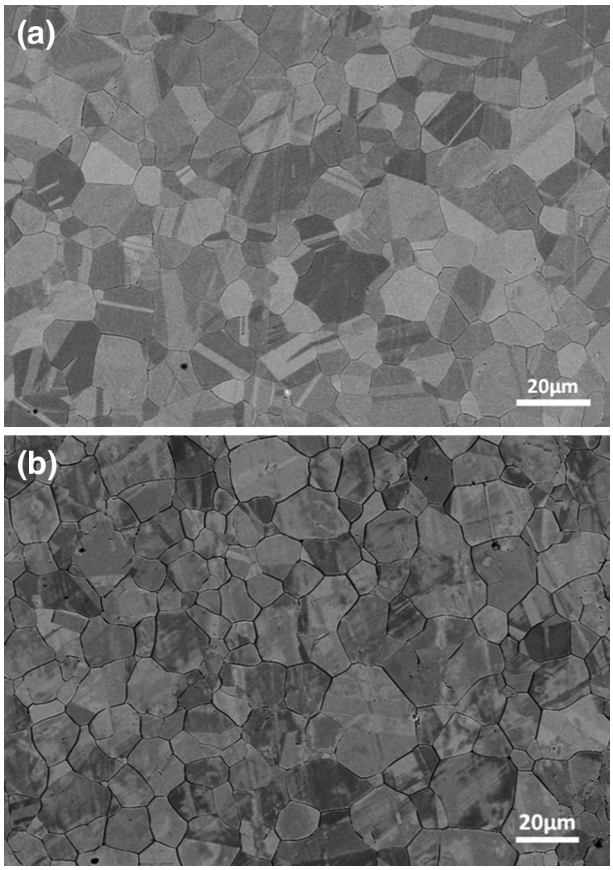

Fig. 1—Typical microstructure of the alloys tested in this work: (*a*) alloy 718 and (*b*) model 718-Nb.

tensile test with serrations, the fracture surface is entirely transgranular ductile, as illustrated in Figure 3.

The gathered data first allow drawing the map shown in Figure 4, representing in the strain rate *vs* temperature plane the locus of PLC and non PLC (DSA) domains. The SEM observations of the fracture surfaces of the specimens for each tensile test allowed to estimate the ratio of intergranular brittle area over the transgranular area. These surface fraction values were reported as numbers (in pct) next to the points in Figure 4. All the tests corresponding to the PLC domain exhibit purely transgranular fracture surface so that the intergranular area proportion was zero, and this was not indicated close to the corresponding points (open circles) in Figure 4. This plot confirms the coincidence between the deformation regime and rupture mode.

In addition, the plastic strain onset ε_c for which the first serration occurs was systematically measured. For a given strain rate, the value of ε_c evolves when the test temperature varies. When the ε_c values decrease with increasing of tensile test temperature, this is called the "normal" behavior. By contrast, when the values of ε_c increase with increasing temperature, the behavior is called "inverse." These two trends of the evolution of the plastic strain onset to the first serration ε_c are illustrated by Figure 5. The temperature of the transition from normal to inverse behavior of ε_c evolves as a function of strain rate.

The experimental data have been plotted on $\ln \dot{\varepsilon}$ *vs* $1/T$ and $\ln \varepsilon_c$ *vs* $1/T$ diagrams for a better view on the domains of existence of PLC effect, and normal/inverse behavior, as shown, respectively, in Figures 4 and 5.

IV. RESULTS ANALYSIS

Various methods have been used in this study to estimate the apparent activation energies of PLC effects in normal and inverse domains that have been widely used and described in other studies; see for instance.[9,17,23,24]

A. *Arrhenius Method*

The temperature and the strain rate dependence of the occurrence of serrated flow are linked by an Arrhenius-like relationship:

$$\dot{\varepsilon} = \dot{\varepsilon}_0 \exp\left(-\frac{Q}{RT}\right), \qquad [1]$$

where Q is the activation energy, R is the gas constant, and T is the temperature.

The slope of the boundary between the domains of the absence and occurrence of PLC effect on a $\log(\dot{\varepsilon})$ *vs* $1/T$ plot is linked to the value of Q_{dis} by the relationship $Q_{dis} = -1/\log(e) \times \text{slope} \times R$. Such a representation is shown on Figure 4 by the solid line.

This representation of DSA and PLC domains leads to an apparent activation energy 320 kJ/mol for the boundary between DSA and PLC occurrence domain. The activation energy calculated for the disappearance Q_{dis} of serrated flow at high test temperature is often considered to be the sum of the activation energy for diffusion of the solute species Q and a quantity linked to the binding energy of solute to dislocation; W, as defined by Cottrell and Bilby[15,25]:

$$W = \frac{4}{3}\frac{G\epsilon r^3(1+\nu)}{1-\nu} \qquad [2]$$

in which $\epsilon = \frac{r_s - r}{r}$; G the shear modulus, ν the Poisson ratio, r_s the solute radius, and r the nickel radius. For further calculations of W, we used an average shear modulus on the range of temperatures, $\bar{G} = 67\,\text{GPa}$,

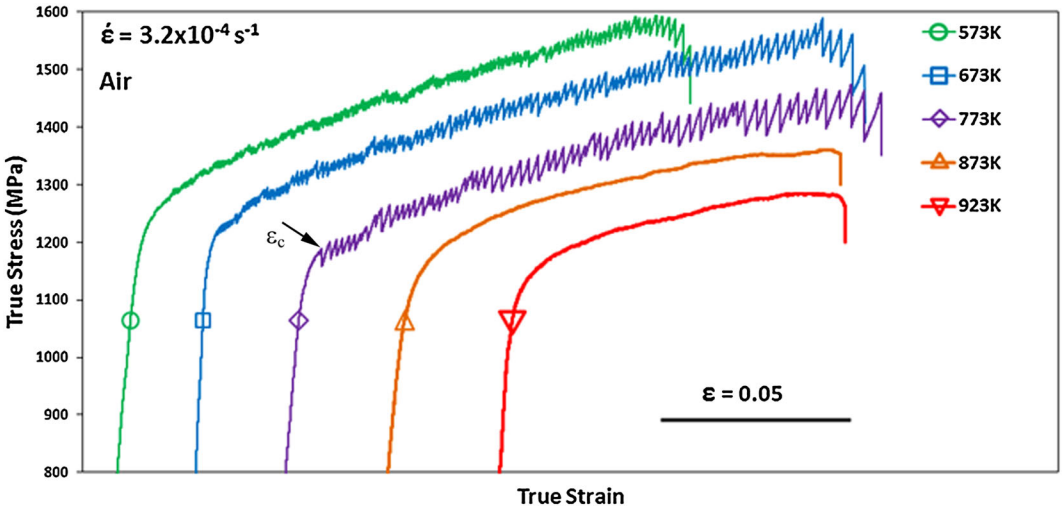

Fig. 2—True stress–true strain curves at $\dot{\varepsilon} = 3.2 \times 10^{-4}\ s^{-1}$ for various temperatures showing the serrated behavior. The critical strain for the onset of the first serration ε_c is shown on 773 K (500 °C) curve. The curves are offset from each other for better visualization.

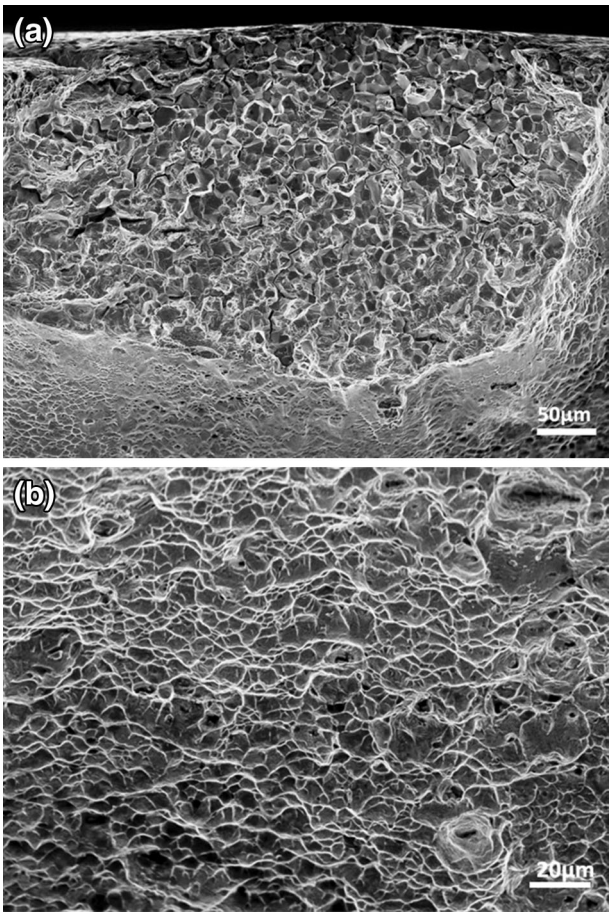

Fig. 3—Rupture surface of a tensile specimen of alloy 718 tested at 873 K (600 °C) in air: (*a*) in the DSA domain-($3.2 \times 10^{-4}\ s^{-1}$), and (*b*) in the PLC domain ($10^{-3}\ s^{-1}$) showing, respectively, the partially intergranular brittle cracking and fully transgranular ductile features.

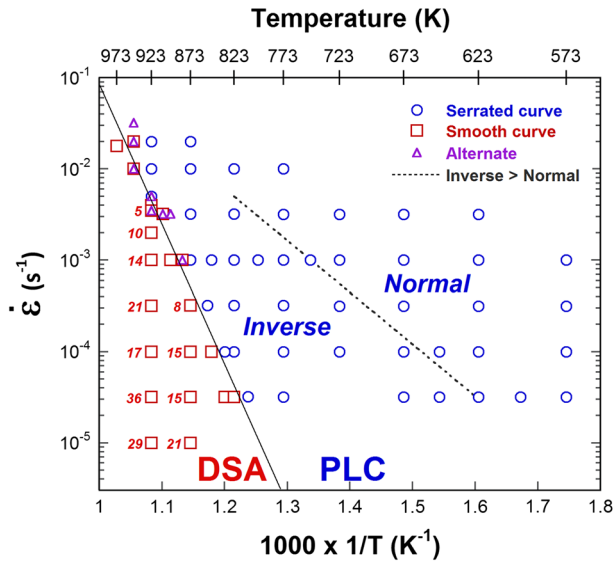

Fig. 4—Map of plastic deformation mechanisms in the temperature-strain rate plane. PLC denotes the domain in which serrated flow is observed (with either normal or inverse behavior of ε_c—see text), and DSA refers to the domain where no serration was observed. Italic numbers close to the open square marks represent the brittle intergranular area proportion on the rupture surface for corresponding tensile test (see text).

Poisson ratio $\nu = 0.3$, and the data for atomic radii of nickel and the different substitutional solute elements constitutive of the alloy that were taken from Reference 26. Hence, the binding energy of the different solutes to dislocations, W, is ranging from 0.4 to 28.8 kJ/mol. Considering the works from Louat[27] who has shown that the slope of the boundary of disappearance of instabilities on a $(\ln \dot{\varepsilon}, 1/T)$ diagram is $Q_{dis} = Q + \frac{3}{2}W$, we obtain an activation energy range for the diffusion of the atomic element involved in this domain of PLC effect which is 277 to 320 kJ/mol. The representation of the frontier between normal and inverse behaviors of ε_c may give information about the transition in mechanisms involved in the serrated flow phenomena. The apparent activation energy obtained from the slope of the dashed line separating normal and inverse PLC domain is about 109 kJ/mol. This energy which corre-

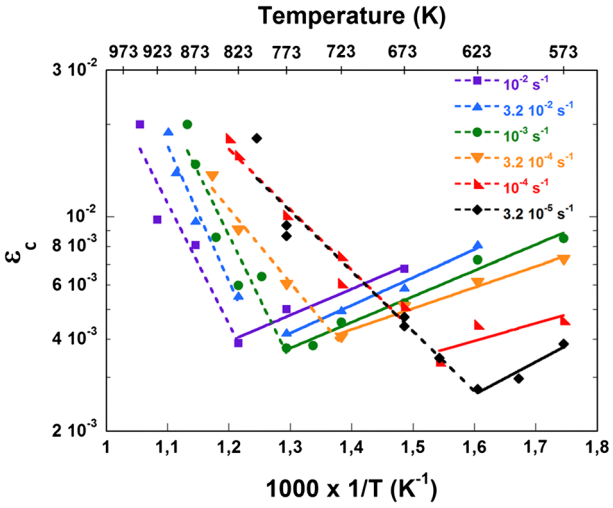

Fig. 5—Variation of the critical strain ε_c for the onset of serrations with temperature for given strain rates. The straight lines show normal domain, while the dot lines show inverse domain.

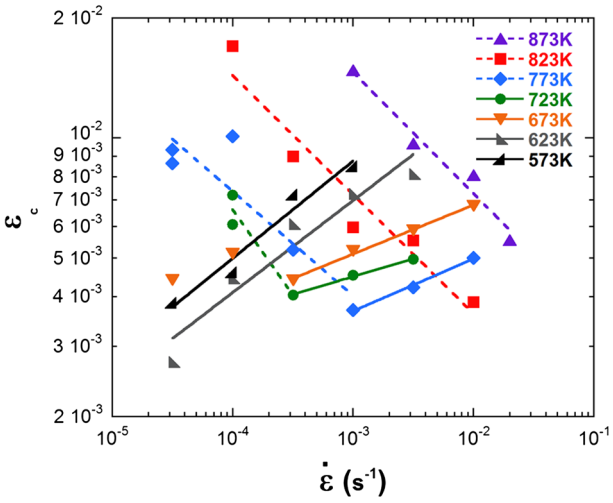

Fig. 6—Variation of the critical strain ε_c for the onset of serrations with strain rate for given temperatures. The straight lines show normal domain, while the dot lines show inverse domain.

Table II. Individual Values of $m + \beta$ Coefficients Determined *Via* the Slopes of $\log \varepsilon_c$ *vs* $\log \dot{\varepsilon}$ for Each Tested Temperature

T (°C)	600	550	500	450	400	350	300
$(m + \beta)_{\text{Inverse}}$	−3.17	−3.39	−4.46	−2.02	—	—	—
$(m + \beta)_{\text{Normal}}$	—	—	9.7	11.17	11.08	4.02	3.94

sponds to the transition between two heat-activated mechanisms might be a weighted average value of the activation energies for diffusion of the species involved in both domain of PLC effect.

B. *Critical Strain Method*

The investigations around serrated flow suggest that the measurement of the critical strain for the onset of serrations, and its dependence on strain rate and temperature is an important parameter for the apparent activation energy calculation. This dependence can by expressed by[28]

$$\varepsilon_c^{(m+\beta)} = K\dot{\varepsilon} \exp\left(\frac{Q}{RT}\right), \qquad [3]$$

where m and β are the respective exponents involved in the variation of vacancies concentration ($C_v \propto \varepsilon^m$) and mobile dislocations density ($\rho_m \propto \varepsilon^\beta$) as a power law of plastic strain, K is a constant.

The following two methods for calculating the apparent activation energies of the PLC effect involve determining first the $(m + \beta)$ exponents of Eq. [3]. The exponents $(m + \beta)$ can be obtained measuring the slope of a plot of $\log(\dot{\varepsilon})$ *vs* $\log(\varepsilon_c)$ at constant temperature. Such a plot is presented in Figure 6. Table II gives the individual values of $m + \beta$ coefficient for each temperature. It may be noticed that the $(m + \beta)$ values obtained in the normal domain are rather scattered and much higher than what is often reported.[29] Nevertheless, using average values of $(m + \beta)$ on different temperature intervals, calculation of apparent activation energies have been carried out that led to values consistent with other methods not using such coefficient as presented below.

Considering Eq. [3], the slope of a plot $\ln(\varepsilon_c)$ *vs* $1/T$ at constant $\dot{\varepsilon}$ permits to obtain a value of Q, as $Q = \text{slope} \times (m + \beta) \times R$. This method involves using an average value of $(m + \beta)$ over a range of $\dot{\varepsilon}$ and T values. Different ranges of temperatures were chosen corresponding to different $(m + \beta)$ average values. The plot used to calculate these slopes is shown in Figure 5.

The results of activation energies obtained by this method in the domain of normal behavior of ε_c are between 43 and 102 kJ/mol. The same method has been applied in order to determine activation energies in the domain of inverse behavior. The activation energies obtained in this domain are between 177 and 277 kJ/mol. The scatter of activation energies values obtained in both normal and inverse domains of evolution of ε_c is quite strong. This is the reason why other methods for the determination of Q have been used to evaluate the effective activation energies for the mechanisms involved in serrated flow in both domains.

C. *McCormick Method*

Another method often used for the determination of activation energies of the PLC effect is the quasi-static aging model developed by McCormick,[30] described by

$$\varepsilon_c^{m+\beta}/T = \dot{\varepsilon}\left(\frac{C_1}{\alpha C_0}\right)^{3/2} \frac{R\mathbf{b}}{LNWD_0} \exp\left(\frac{Q}{RT}\right), \qquad [4]$$

where C_0 is the initial concentration of the solute in the alloy, C_1 is the local concentration of the solute nearby the dislocation, L is the obstacle spacing, W is the maximum solute-dislocation interaction energy, D_0 is the diffusion frequency factor, $\mathbf{b}$ is the Burger's vector, and N is a constant. Using the previous equation,

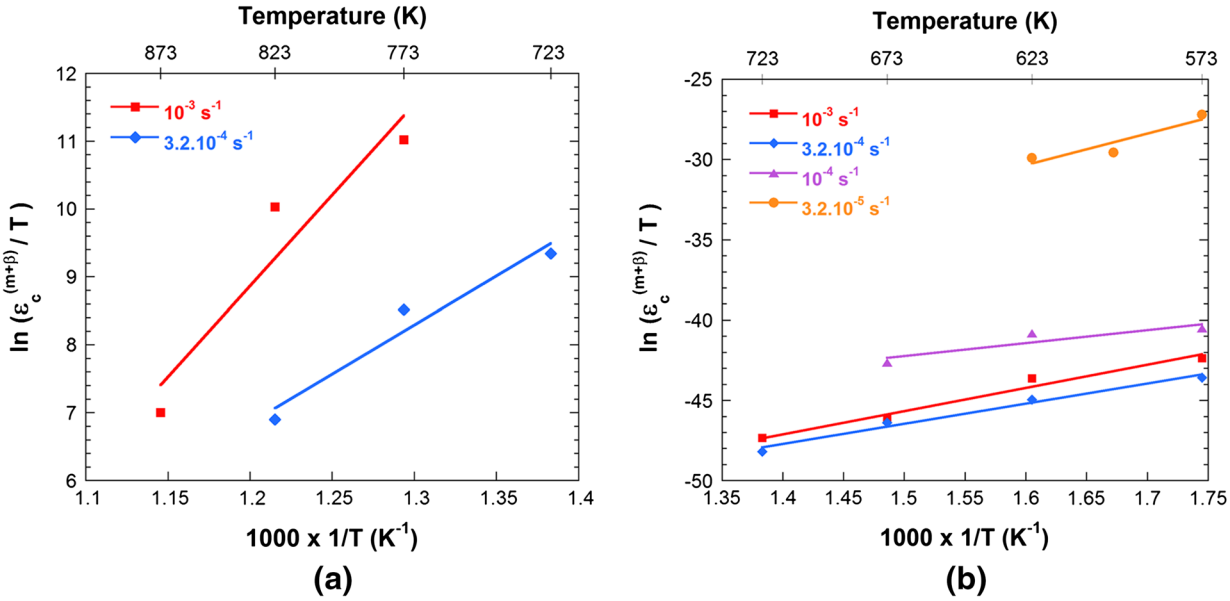

Fig. 7—Plots of $\log(\varepsilon_c^{(m+\beta)}/T)$ *vs* $1/T$ for (*a*) inverse and (*b*) normal behavior of ε_c.

Chaturvedi and Kim[18] have evaluated Q for given $\dot{\varepsilon}$ values from the slope of the plot $\ln(\varepsilon_c^{m+\beta}/T)$ *vs* $1/T$, with $Q = \text{slope} \times R$.

This method has been applied in the present study for different strain rate values in the normal and inverse domains. Whereas this method would allow using individual values of $(m + \beta)$ exponents for each $(\dot{\varepsilon}, T)$ couple, the scatter of the exponents determined in the present study lead to use average $(m + \beta)$ values over different temperature ranges. The plots used to determine these activation energies are shown in Figure 7.

The activation energies obtained *via* this method gives values that are 66 to 162 kJ/mol in the normal domain and 120 to 223 kJ/mol in the inverse domain.

D. *Intercept Method*

In their works on DSA in a Cu-Sn alloy, Qian and Reed-Hill[31] suggested that the methods of determination of the activation energy based on Cottrell and McCormick models require unverifiable assumptions on the evolution of ε_c with dislocations density and vacancies concentration during plastic deformation. This is why they proposed a method to determine the apparent activation energy for PLC effect at given ε_c. This method can be called the intercept method. From the plots $\ln(\dot{\varepsilon})$ *vs* $\ln(\varepsilon_c)$ (Figure 6) at various temperatures, different levels of critical strain as a function of $(\dot{\varepsilon}, T)$ couples can be obtained. Reporting these values on a $\ln(\dot{\varepsilon})$ *vs* $1/T$ diagram for different critical strain levels generates a set of lines, which slopes are linked to the value of Q by the relationship $Q = \text{slope} \times R$.[23] One of the interests of this method is that it does not involve the use of $(m + \beta)$. The couples $(\dot{\varepsilon}, T)$ generating a given ε_c have been determined and plotted on a $\ln(\dot{\varepsilon})$ *vs* $1/T$ diagram, as shown on Figure 8.

This method was applied to determine the apparent activation energies for each domain. The values of activation energies obtained by the intercept method are of 85 to 114 kJ/mol for the PLC effect in the normal domain, and 244 to 248 kJ/mol in the inverse domain.

E. *Serration Amplitude Method*

Hayes and Hayes,[17] as well as Pink and Grinberg,[24,32] also suggested that Q can be obtained from load drops measurement. The stress drop accompanying serrated flow is measured at a given strain for a range of $\dot{\varepsilon}$ and T, and is reported on a $\Delta\sigma = f(\dot{\varepsilon})$ plot for different temperature values. A constant value of $\Delta\sigma$ is then selected from which the corresponding $\dot{\varepsilon}$ is determined for each temperature. The resulting $(\dot{\varepsilon}, T)$ couples are then reported on an $\dot{\varepsilon} = \text{f}(1/\text{T})$ plot. Q is determined from the slope of this plot, as $Q = -1/\log(e) \times \text{slope} \times R$

In this method, an average value of the amplitude of the stress drop has to be measured for each tensile test from the true stress–true strain curve at a constant plastic strain value, which was set to $\varepsilon_p = 5$ pct in the present study. The evolution of 5 pct plastic strain-stress drops amplitude as a function of $\dot{\varepsilon}$ is plotted on Figure 9, for different temperatures.

This method consists then in determining the couples $(\dot{\varepsilon}, T)$ generating some arbitrarily chosen magnitudes of stress drops. The chosen stress drops values have been 40 and 50 MPa for inverse domain and 15 and 20 MPa for the normal domain. The corresponding $(\dot{\varepsilon}, T)$ couples have then been plotted on a $\log(\dot{\varepsilon})$ *vs* $1/T$ diagram shown in Figure 10. The values obtained for the activation energies are about 71 to 89 kJ/mol for the normal domain and 110 to 124 kJ/mol for the inverse domain.

Table III summarizes the results of the calculations of activation energies by the different methods previously presented. The apparent activation energies calculated in both domains are rather dispersed, but an obvious

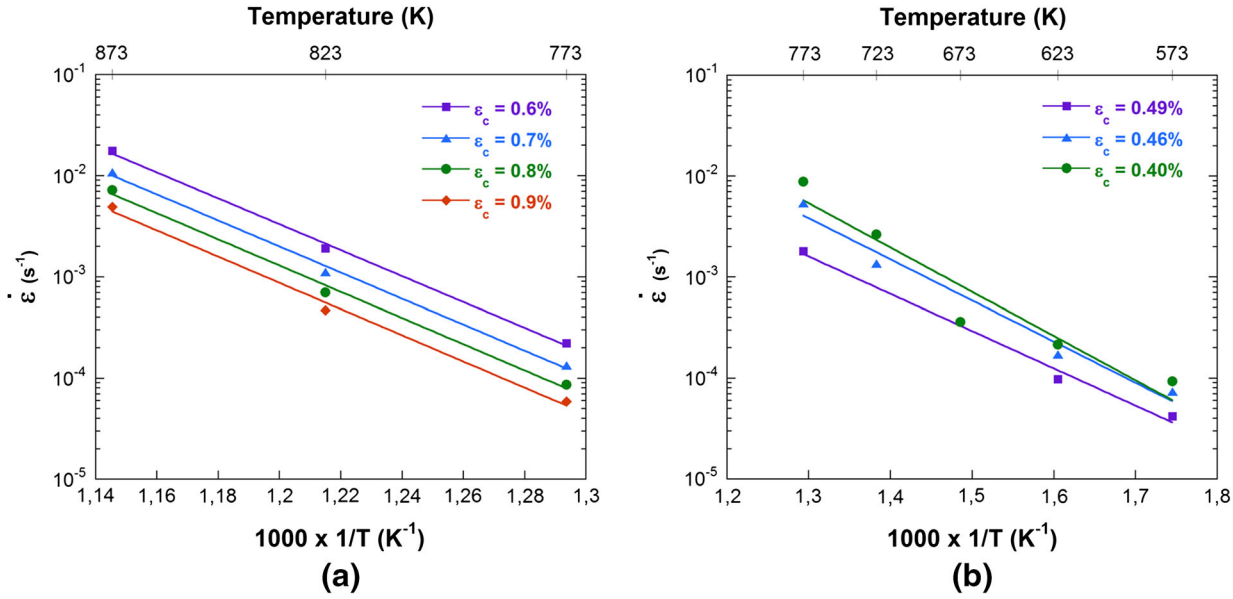

Fig. 8—Plots of strain rate and temperature producing given critical strains ε_c for (*a*) inverse and (*b*) normal behavior of ε_c.

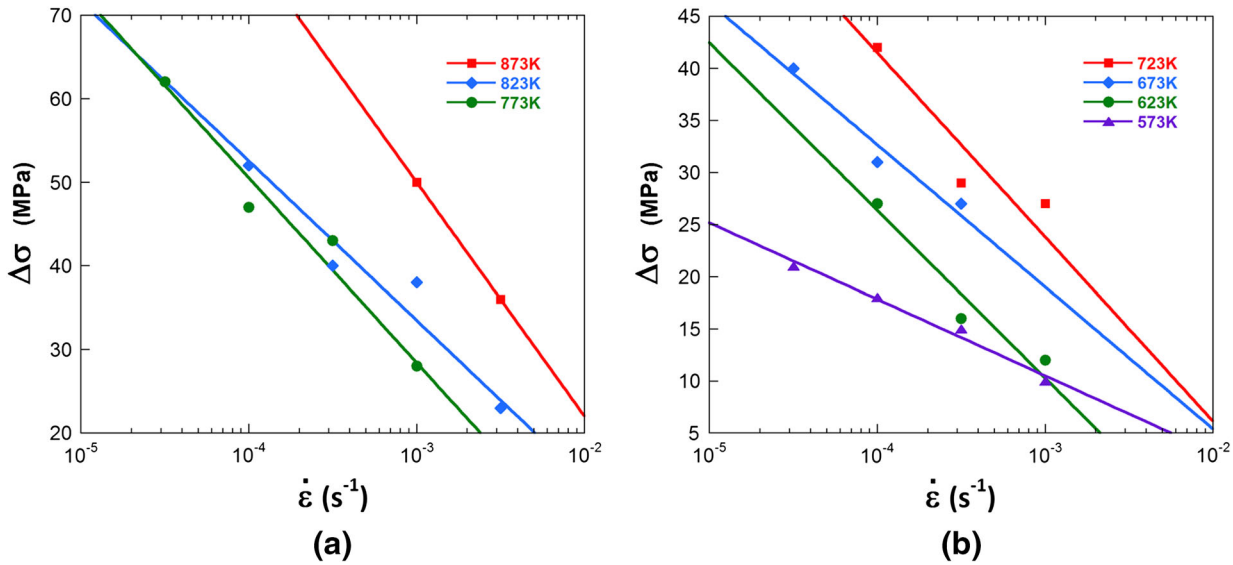

Fig. 9—Variation of the magnitude of stress drops at 5 pct plastic deformation as a function of strain rate for given temperatures (*a*) for inverse and (*b*) for normal behavior of ε_c.

difference appears when considering a representative value of Q for each domain. It is thus considered that in the normal domain, a representative range of apparent activation energies for the occurrence of PLC effect is 80 to 100 kJ/mol, while in the inverse domain, the range is approximately 200 to 280 kJ/mol.

V. DISCUSSION

A. *Preliminary Considerations*

Before discussing the results obtained in the present study, it must be emphasized that the PLC phenomenon effects on the macroscopic tensile curve may strongly depend on the metallurgical state of the 718 alloy. In the present study, the alloy 718 had been aged following the conventional aeronautical route: solutionning and aging at 993 K (720 °C)/8 h and 893 K (620 °C)/8 h. The corresponding microstructure consists in a very fine γ' and γ'' precipitation and nearly no δ precipitate.[12] This microstructure corresponds, regarding the denomination used in other PLC studies of alloy 718, to an underaged metallurgical state.

The numerous tensile tests performed allowed to draw quite accurately on a strain rate—inverse temperature planes the boundaries for the occurrence domain of PLC serrations. Additionally, this PLC domain could be shared between normal and inverse behavior for the

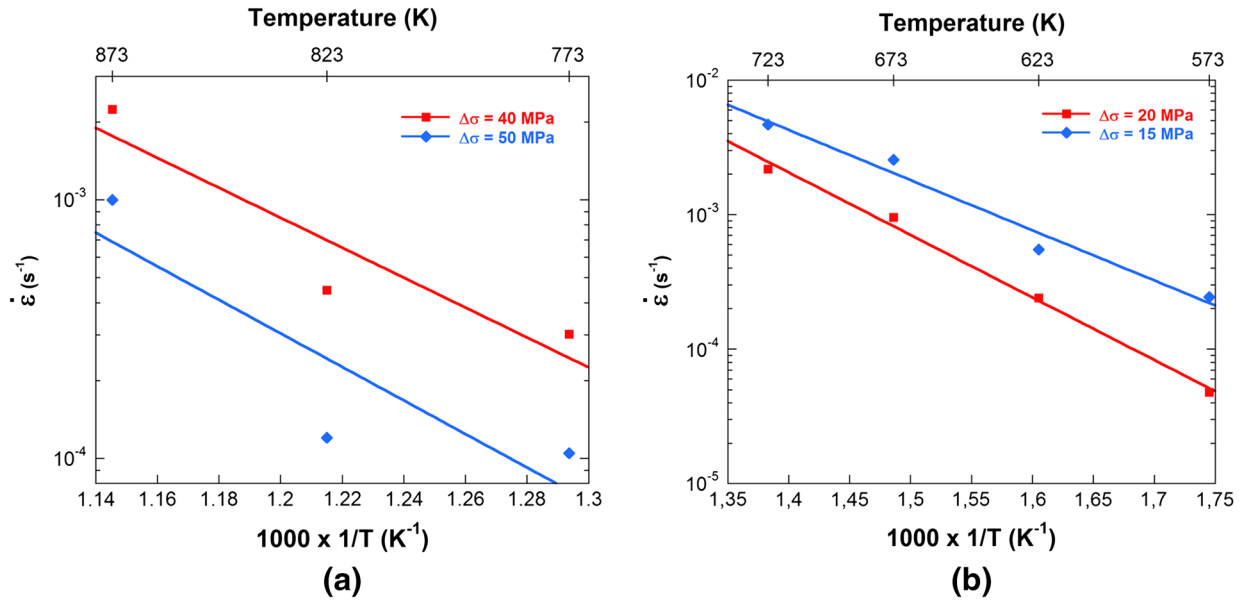

Fig. 10—Plots of strain rate and temperature couples producing given magnitudes of 5 pct plastic deformation stress drops for (*a*) inverse and (*b*) normal behavior of ε_c.

Table III. Summary of the Apparent Activation Energies Calculated by Different Methods for Low Temperature (Normal) and High Temperature (Inverse) PLC Effect

	Action Energies (kj/mol)	
Method	Normal	Inverse
Arrhenius	109	276 to 320
Critical strain	43 to 102	177 to 277
Intercept	76 to 103	244 to 248
McCormick	66 to 162	120 to 233
Stress drops	71 to 89	110 to 124

evolution of the critical strain to the onset of the serrations. From this map, various methods were employed to calculate the apparent activation energies of the mechanisms involved in both normal and inverse PLC regimes. Representative values of apparent activation energies obtained in this study are approximately 80-100 kJ/mol for the low temperature (normal) PLC effect, and 200 to 280 kJ/mol for the high temperature (inverse) PLC effect, which is fully consistent with previous studies on the alloy.[6,9,10]

B. *Identification of Solute Elements Involved in DSA*

A common way to try identifying the solute species involved in the occurrence of the PLC effects is to compare the calculated apparent activation energies in each domain with the activation energies for the diffusion of various solute species in the alloy. An abundant literature on diffusion data of various species in Ni and Ni-based alloys exists. The reader may refer to the following papers for diffusion data.[9,33–35] The comparison of these values with the apparent activation energies for PLC effect determined by various methods in this study is consistent with what has been published by different authors for this alloy.

Concerning low temperature PLC effect, activation energy is of the order of 80-100 kJ/mol which is comparable to the activation energies for lattice and pipe diffusion of C atoms in Ni-based alloys. The origin of the low temperature PLC effect seems to be well accepted by the community: indeed, since the works from Nakada and Keh[36] on binary Ni-C alloys and those from Blakemore,[37] a general consensus have imposed concerning the origin of low temperature PLC effect in most Ni-based alloys and superalloys. Low temperature PLC effect is attributed to the interaction between carbon atmosphere and mobile dislocations during plastic deformation in alloy 718 as assumed by, Hayes,[6] Chen and Chaturvedi,[8] Hale *et al.*,[9] Nalawade *et al.*,[10] and in other Ni-based alloys see *e.g.*, Hrutkay and Kaoumi.[38]

Regarding high temperature PLC effect, the value of activation energy determined in this study is 200 to 280 kJ/mol. This energy range fits pretty well with the diffusion energy of the main substitutional solute species in alloy 718 (Cr, Fe, Mo, and Nb) according to previous experimental results[9] (see also a review in Reference 39) or calculated values.[40] Indeed, the occurrence of jerky flow has been ascribed to the effect of Cr,[9] Nb[6,10] in alloy 718, and to Mo[18] in an alloy 625. However, following considerations of Cottrell's work,[6,10] the occurrence of jerky flow is related to diffusion energy, but also to solute-dislocation binding energy W. This later value being directly linked to solute *vs* matrix atom sizes (see Eq. [2]). Consequently, most attention is paid on the role of Nb and Mo, which were shown to most expand the Ni cell size.[41] Hayes[6] attributed high temperature PLC phenomenon to the effect of Nb, proposing that the disappearance of serrations at high strains results from the solutes depletion of the dislocations atmospheres by the formation of NbC fine clusters during plastic deformation. More recently, Nalawade

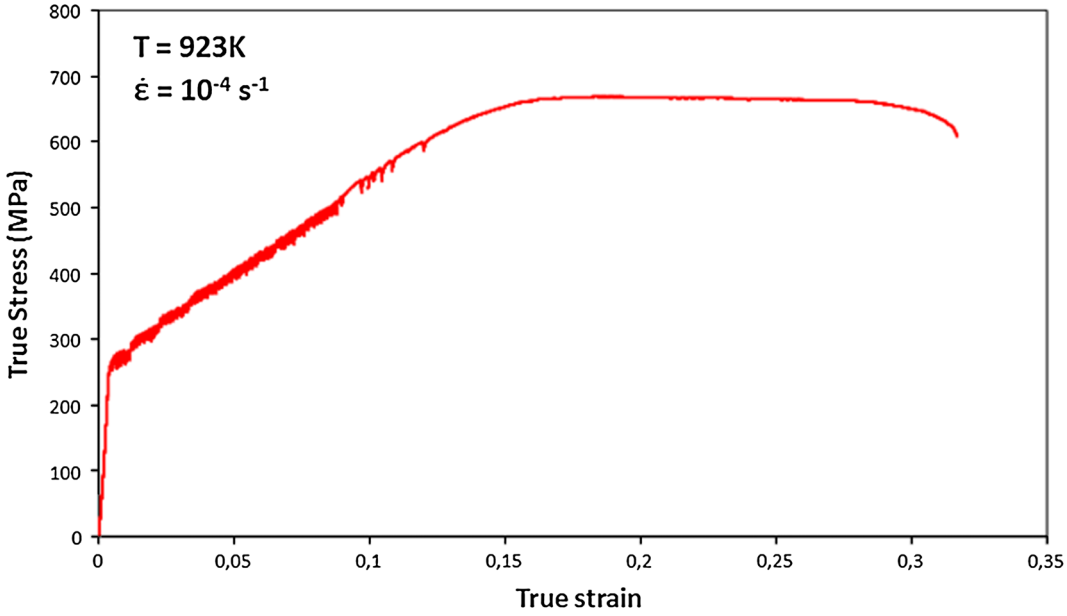

Fig. 11—True stress–true strain curve of a model alloy 718-like without Nb exhibiting PLC effect for testing conditions 923 K (650 °C) to 10^{-4} s^{-1}.

et al.[10] compared the serrated behavior of alloy 718 for different metallurgical states. In particular, they observed that the temperature for the PLC to DSA transition is higher for solid solution treated alloy [973 K (700 °C)] as compared to the temperature for either γ'' or δ precipitates states [823 K (550 °C)]. They concluded that the PLC domain is extended toward high temperatures with the increase of solute Nb atoms. The high temperature PLC effect in alloy 718 was thus attributed to the interaction between Nb and mobile dislocations. Moreover, based on the 3D atom probe tomography results from Miller *et al.*[42] Nalawade *et al.*[10] ruled out the possibility that Mo might be responsible for high temperature jerky flow. In order to evaluate the effect of Nb on the serrated behavior of alloy 718, we carried out tensile tests on a model alloy 718-like but without Nb (Alloy 718-Nb), which composition is given in Table I. This alloy is in a solid solution state and was tensile tested in a domain of temperatures and strain rates where high temperature PLC effect can occur [*i.e.*, 923 K (650 °C)/10^{-4} s^{-1}]. These tensile tests exhibited serrated flow that extends over more than 10 pct plastic strain despite the alloy is niobium-free, as shown on Figure 11. This experimental result shows that plastic flow instabilities can occur in the solid solution state of the alloy without Nb. This means that Nb cannot be considered as the only responsible for the occurrence of PLC effect in the inverse domain for alloy 718 and thus highlights the possible role played by Mo atoms.

C. *Displacement of the PLC Effect Domain*

Concerning the disappearance of the PLC effect for high testing temperatures, a study carried out by Ter-Ovanessian *et al.*[13] has shown that for the same heat of alloy 718, lowering the interstitials content tends to extend the PLC effect domain toward high temperatures and slow strain rates. The heat treatments applied to reduce the interstitial content [1253 K (980 °C)-15 h/30 h] led to the precipitation of delta phase in the alloy. Nevertheless, Nalawade *et al.*[10] showed that delta precipitation would tend to move the DSA/PLC boundary toward lower temperature. Hence, interstitial elements, whereas they are not directly responsible for high temperature PLC effect by interacting with dislocations, seem to have a strong influence on the extent of the domain where PLC effect occurs. The fact that PLC domain extends when the interstitial content is reduced means that the breakaway of dislocations from their atmospheres occurs for higher temperature and slower strain rates, so that the atmosphere dragged behind the dislocations has a reduced mobility. This can be understood in terms of competition between solute species for forming part of the dislocation atmospheres: hence, the reduction of mobility can be due to the nature of the atmosphere, which may be constituted of heavier atomic species, mostly substitutional ones in the case of low interstitial content. On the contrary, when the interstitial content is high, the available sites in the tension stress field near the dislocation cores are fewer and less accessible to substitutional elements due to the important concentration of interstitial atomic elements that are dragged behind the mobile dislocations in this domain of temperatures and strain rates.

D. *Considerations on Inverse Behavior*

The existence of an inverse domain for the evolution of ε_c has been considered by Brechet and Estrin[43] to be the result of precipitation during plastic deformation. This phenomenon is more likely to occur during plastic deformation as diffusion is strongly enhanced in the area surrounding dislocations where the lattice is distorted.

This is the reason why co-precipitation of complexes between interstitial and substitutional elements involved in both types of PLC effect, *i.e.*, "low temperature" and "high temperature," may be active while these species are transported in the strain field of mobile dislocations or at the forest dislocation nodes at which mobile dislocations are arrested. This formation of complexes tends to reduce the capacity of the atomic elements to move, as they become tied up together. This can explain why the behavior of ε_c is inverse for high testing temperatures: the complexation becoming more and more effective with temperature, the cumulated plastic strain required to form an atmosphere which average mobility is compatible with dislocations velocity increases. Hence, the occurrence of serrated flow requires more important deformation as substitutional-interstitial complexes tend to form in the early stages of the specimen straining until the atmosphere reaches a composition which enables it to diffuse with a critical velocity compatible with a dynamic interaction with mobile dislocations and the occurrence of serrated flow.

E. *Relation with Intergranular Cracking*

The fracture mode sharp transition previously identified in this alloy fits with the boundary between DSA and inverse behavior domain. This experimental fact might be explained as follows: Oxidation-assisted intergranular crack initiation requires a local intergranular strain rate slow enough to be compatible with intergranular oxidation process. In the case of PLC bands, the local strain rate is too high to be compatible with intergranular oxidation process so that crack initiation cannot occur. Nevertheless, it has been found in a previous study[13] that reducing the carbon content in a given heat led to a decrease of the intergranular crack initiation sensitivity of alloy 718 in this temperature range as well as a displacement of the boundary between the DSA and PLC regimes occurrence domains. Below a critical carbon content and even for slow strain rate the alloy seemed to be insensitive to the oxidation-assisted intergranular crack initiation. Thus, interactions between solute elements *i.e.*, interstitial and substitutional, are suspected to contribute to the crack initiation process.

VI. CONCLUSIONS

The great number of mechanical tests carried out in the present study allowed to confirm that two domains of PLC instabilities, namely normal and inverse behavior of critical strain ε_c with temperature, can be distinguished in the investigated temperature and strain rates ranges. These two domains are characterized by significantly different apparent activation energies associated with, respectively, interstitial or substitutional solute elements interaction with mobile dislocations. Our results confirm that the interstitial species involved may be mainly carbon, whereas the substitutional atoms responsible for inverse domain are still not unambiguously determined. Indeed, we show that serrations occur even in the absence of niobium which indicates that the role of substitutional element such as molybdenum cannot be ruled out. Complementary studies based on both mechanical spectroscopy and Density Functional Theory calculations are undertaken to investigate the relevancy of this hypothesis. From a macroscopic point of view, the disappearance of oxidation-assisted intergranular cracking within the PLC domain may be associated to the highly localized strain bands generating very high local strain rate non compatible with intergranular oxidation kinetics.

REFERENCES

1. J. Pedron and A. Pineau: *Mater. Sci. Eng.*, 1982, vol. 56, pp. 143–56.
2. E. Andrieu, R. Molins, H. Ghonem, and A. Pineau: *Mater. Sci. Eng. A*, 1992, vol. 154, pp. 21–28.
3. M. Miglin and H. Domian: *J. Mater. Eng.*, 1987, vol. 9, pp. 113–32.
4. R. Wanhill: *Int. J. Fatigue*, 2002, vol. 24, pp. 545–55.
5. J. Deleume: Ph.D. Thesis, Institut National Polytechnique de Toulouse, 2007.
6. R.W. Hayes: *Acta Metall.*, 1983, vol. 31, pp. 365–71.
7. H. Dybiec: *Arch. Metall. (Pol.)*, 1991, vol. 36, pp. 341–52.
8. W. Chen and M.C. Chaturvedi: *Mater. Sci. Eng.*, 1997, vol. A229, pp. 163–68.
9. C.L. Hale, W.S. Rollings, and M.L. Weaver: *Mater. Sci. Eng.*, 2001, vol. A300, pp. 153–64.
10. S.A. Nalawade, M. Sundararaman, R. Kishore, and J.G. Shah: *Scripta Mater.*, 2008, vol. 59, pp. 991–94.
11. L. Fournier, D. Delafosse, and T. Magnin: *Mater. Sci. Eng.*, 2001, vol. A316, pp. 166–73.
12. V. Garat, J.-M. Cloué, D. Poquillon, and E. Andrieu: *J. Nucl. Mater.*, 2008, vol. 375, pp. 95–101.
13. B. Ter-Ovanessian, J. Deleume, J.-M. Cloué, and E. Andrieu: *Mater. Sci. Forum*, 2008, vols. 595–598, pp. 951–58.
14. A. Yilmaz: *Sci. Technol. Adv. Mater.*, 2011, vol. 12, pp. 1–16.
15. A. Cottrell and B. Bilby: *Proc. Phys. Soc. Lond. A*, 1949, vol. 62, pp. 49–62.
16. A. Cottrell: *Philos. Mag.*, 1953, vol. 44, pp. 829–32.
17. R.W. Hayes and W.C. Hayes: *Acta Metall.*, 1982, vol. 30, p. 1295.
18. M.C. Chaturvedi and I.S. Kim: *Trans. Jpn. Inst. Met.*, 1987, vol. 28 (3), pp. 205–12.
19. V. Shankar, M. Valsan, K. Bhanu Sankara Rao, and S.L. Mannan: *Metall. Mater. Trans. A*, 2004, vol. 35A, pp. 3129–39.
20. K. Gopinath, A.K. Gogia, S.V. Kamat, and U. Ramamurty: *Acta Mater.*, 2009, vol. 57, pp. 1243–53.
21. M. Mazière, J. Besson, S. Forest, B. Tanguy, H. Chalons, and F. Vogel: *Eur. J. Comput. Mech.*, 2008, vol. 17, pp. 761–72.
22. S.A.R. Sharghi-Moshtaghin: *Mater. Sci. Eng.*, 2008, vol. 486A, pp. 376–80.
23. S. Venkadesan, C. Phaniraj, P.V. Sivaprasad, and P. Rodriguez: *Acta Metall.*, 1992, vol. 40, pp. 569–80.
24. E. Pink: *Scripta Metall.*, 1983, vol. 17, pp. 847–52.
25. A.H. Cottrell: *Rep. Conf. Strength Solids*, 1947, pp. 30–36.
26. M.C. Ball and A.H. Norbury: *Physical Data for Inorganic Chemists*, Longman, London, 1974.
27. N. Louat: *Scripta Metall.*, 1981, vol. 15, pp. 1167–70.
28. A. Van den Beukel: *Phys. Status Solid*, 1975, vol. 30, pp. 197–206.
29. A. van den Beukel: *Acta Metall.*, 1982, vol. 28, pp. 965–69.
30. P.G. McCormick: *Acta Metall.*, 1972, vol. 20, pp. 351–54.
31. K.W. Qian and R.E. Reed-Hill: *Acta Metall.*, 1983, vol. 31, pp. 87–94.
32. E. Pink and A. Grinberg: *Mater. Sci. Eng.*, 1981, vol. 51, pp. 1–8.
33. M.S.A. Karunaratne and R.C. Reed: *Defect Diffus. Forum*, 2005, vol. 308, pp. 2–10.
34. D. Pruthi, M. Anand, and R. Agarwala: *J. Nucl. Mater.*, 1977, vol. 64, pp. 206–10.

35. R. Swalin and A. Martin: *J. Met*., 1956, vol. 8, pp. 567–72.
36. Y. Nakada and S. Keh: *Acta Metall*., 1970, vol. 18, pp. 437–43.
37. J.S. Blakemore: *Metall. Trans*., 1970, vol. 1, pp. 1281–85.
38. K. Hrutkay and D. Kaoumi: *Mater. Sci. Eng*., 2014, vol. 599, pp. 196–203.
39. B. Max: PhD. Thesis, Institut National Polytechnique de Toulouse, 2014.
40. C.L. Fu, R. Reed, A. Janotti, and M. Krcmar: *Superalloys*, 2004, vol. 2004, pp. 867–76.
41. A. Jena and M. Chaturvedi: *J. Mater. Sci*., 1984, vol. 19, pp. 3121–39.
42. M.K. Miller, S.S. Babu, and M.G. Burke: *Mater. Sci. Eng. A*, 2002, vol. A327, pp. 84–88.
43. Y. Brechet and Y. Estrin: *Acta Metall. Mater*., 1995, vol. 43, pp. 955–63.